Summer 2021

Ground Control Point Assessment for sUAS-based SfM Photogrammetry

Bailey Dianne Wolf
Missouri State University, Bailey230@live.missouristate.edu

GROUND CONTROL POINT ASSESSMENT FOR SUAS-BASED SFM PHOTOGRAMMETRY

A Master's Thesis

Presented to

The Graduate College of

Missouri State University

In Partial Fulfillment

Of the Requirements for the Degree

Master of Science, Geography & Geology-Geospatial Sciences

By

Bailey D. Wolf

July 2021

GROUND CONTROL POINT ASSESSMENT FOR SUAS-BASED SFM PHOTOGRAMMETRY

Geography, Geology and Planning

Missouri State University, July 2021

Master of Science

Bailey D. Wolf

ABSTRACT

The use of small Unmanned Aerial Systems (sUAS) in combination with Structure from Motion (SfM) photogrammetry is an evolving tool for geoscientists. SfM photogrammetry allows for rapid acquisition of the data that is required to create orthophotos and Digital Surface Models (DSMs) for a variety of field applications. Ground Control Points (GCPs) are used to reconstruct the DSM and evaluate the accuracy of aerial imagery collected from sUAS. When acquiring data for SfM photogrammetry, GCPs are required for spatial referencing. However, questions remain open regarding the effect of methodological techniques on the precision and accuracy of the resulting DSMs. This study focuses on assessing the relationship between DSM accuracy and the GCP methodology used to georeference the imagery. By determining the minimal number of GCPs necessary for a specific level of accuracy and precision in the final DSM products, both time and money are saved during data collection and processing.

KEYWORDS: ground control point, structure from motion, photogrammetry, drone, small unmanned aerial system, digital surface model, digital elevation model

GROUND CONTROL POINT ASSESSMENT FOR

SUAS-BASED SFM PHOTOGRAMMETRY

By

Bailey D. Wolf

A Master's Thesis
Submitted to the Graduate College
Of Missouri State University
In Partial Fulfillment of the Requirements
For the Degree of Master of Science, Geography & Geology-Geospatial Sciences

July 2021

Approved:

Toby Dogwiler, Ph.D., Thesis Committee Chair

Xin Miao, Ph.D., Committee Member

Damon J. Bassett, M.S., Committee Member

Julie Masterson, Ph.D., Dean of the Graduate College

ACKNOWLEDGEMENTS

I would first like to thank my advisor Dr. Dogwiler, whose expertise was invaluable in formulating the research question and supporting methodology. Thank you for seeing the potential in this project and for giving me this opportunity.

I would also like to thank each of my professors whose passion for teaching and for science inspired me to embark on this journey. The lessons that I have learned have helped shape who I am today.

I would like to acknowledge my colleagues at the City of Springfield who have shown me great support and pushed me professionally. I would particularly like to thank my supervisors who place immense value on education and allowed me the flexibility to pursue my Masters.

In addition, I would like to thank my family and friends for always being there to offer their ears and advice. I would not have been able to complete this thesis without the happy distractions that allowed my mind to rest outside of my research. Mom, you will never know how much Sunday night dinners mean to me.

I dedicate this thesis to my loving husband, Zach Wolf. Thank you for your never-ending belief in me.

TABLE OF CONTENTS

LIST OF TABLES

LIST OF FIGURES

INTRODUCTION

The utility of small Unmanned Aerial Systems (sUAS) has progressed at a rapid pace in recent years. Prior to the use of sUAS, satellites, manned aircraft, and professional surveillance cameras were the primary methods of data acquisition for aerial imagery [18]. As recent advances have been made, sUAS have proven to be an effective platform for aerial mapping applications. The ability to create high-resolution datasets is a valuable tool that is used to help meet high-resolution topographic dataset production needs [21]. With the ability to access a range of study areas and capture data easily, sUAS have been integrated into a variety of surveying workflows. They have been utilized as an efficient safety inspection and monitoring tool on construction jobsites [16], used to determine crop physiological parameters [15], and used for air quality measurements [14], along with a wide variety of other applications. Without the use of sUAS, the collection process of aerial imagery is much more limited. While there are various aerial platforms to choose from, the use of drones has proven to be an exceptionally reliable and effective option [29].

The data acquired from sUAS is used to construct highly accurate digital surface models (DSMs) [25]. These DSMs provide the basic information for detection and analysis of elevation change. The digital elevation models (DEMs) and orthophotos derived from drone imagery, serve as base maps to design and execute projects [27]. It is typical to analyze DSMs as most real-world drone applications do not generate bare earth, as opposed to DEMs, which can require additional steps to remove vegetation and other ground cover. Knowing the accuracy of the data is a key factor. Previous studies have demonstrated that ground control points (GCPs) are necessary to accurately georeference sUAS products [29]. There is an open issue of achieving

the desired accuracy of DSMs produced using the minimal number of GCPs. As drone technology continues to progress, so does the need for industry standards when it comes to the number and spatial distribution of GCPs. A study to determine the suitable number of GCPs for UAS images georeferencing by varying number and spatial distribution states that there is a minimum of three GCPs which are required to bring the results into a desired coordinate system through the indirect georeferencing process [30]. Since triangulation is used to calculate the relative 3D positions, the three GCPs are needed mathematically. The accuracy of the DSMs produced are assessed by means of root mean square error (RMSE) computation. This statistically represents the errors between the constructed results and the checkpoints [18]. If the value of the index is not as accurate as desired, the process is re-run after increasing the GCP number [26].

Unmanned Aerial Systems

Small Unmanned Aerial Systems. Small Unmanned Aerial Systems (sUAS) are aircraft that do not have a human pilot on board. They are flown remotely by a pilot with a control system or autonomously. These systems were initially developed for military purposes. As technology has rapidly advanced over recent years, they have become more adapted for commercial and civil use. Compared to manned aircraft and satellite remote sensing platforms, sUAS have the capability of on-demand deployment for high resolution data collection at a relatively low-cost [9]. This transformation has made it possible to easily and cost effectively obtain remotely sensed imagery and data.

Multi-Rotor sUAS. The multi-rotor system is a unit which has a constant rotation of rotor blades. Quadcopters control their roll and pitch rotation by adjusting the speed of two motors on one side at a time. The altitude is controlled by adjusting all four of the motors at the

same time. This is what gives it the ability to hover and have a vertical takeoff that does not require a runway. The rotor blades also give the unit a greater range of motion, making them easier to maneuver. Since they are easier to operate, you have the capability to complete more flexible flight missions. However, multi-rotor sUAS do take more power to sustain flight compared to fixed-wing systems which use a wing like a traditional aircraft. The fixed-wing systems do not hold themselves up in the air, making them more energy efficient. Since the multi-rotor has shortened flight times, they typically require multiple flight missions which results in more data collection time in the field. Although you could end up spending more time in the field, you typically spend less money on the multi-rotor unit, and they are lightweight and portable. The Phantom 4 Pro which is shown in **Figure 1** is a multi-rotor system. It is equipped with a 1-inch 20-megapixel camera that has a lens with 24mm focal length and an intelligent flight battery which allows for a flight time of 30 minutes [6].

Figure 1. DJI Phantom 4 Pro Multi-Rotor sUAS and Controller

Photogrammetry

Photogrammetry has been defined by the American Society for Photogrammetry and Remote Sensing as the art, science, and technology of obtaining reliable information about physical objects and the environment through processes of recording, measuring, and interpreting photographic images and patterns of recorded radiant electromagnetic energy and other phenomena [11]. Photogrammetry dates back to as early as 350 B.C. when Aristotle first referred to the process of projecting images optically. Although it was not until the 18th century that J.H. Lambert suggested that these principles could be applied to map making. Once the photographic process was developed in 1839 by Louis Daguerre, the process of photogrammetry was made possible. The first practical application of using photogrammetry for map making was in 1849, using kites and balloons as the method of obtaining aerial photographs. This work was done under the direction of Colonel Laussedat of the French Army Corps of Engineers, who is known as the "father of photogrammetry". Since then, many advances in this process have been made, however the basis of using photogrammetry to produce maps and precise three-dimensional positions of points remains the same. Traditional photogrammetry requires precise knowledge of the 3D location and pose of the camera, along with the precise 3D location of a series of control points in the area [12]. The addition of sensors which are mounted on platforms that make the photogrammetric data acquisition possible are just one example of the many vast improvements to the process of obtaining aerial photographs. Triangulation is then used to reconstruct scene geometry from this information. The tie points in the input photograph are automatically identified by image processing algorithms using the process of "camera pose estimation" to determine the camera position.

Structure from Motion Photogrammetry. Structure from Motion (SfM) is a photogrammetric method for creating three-dimensional models of a feature or topography from overlapping two-dimensional photographs taken from many locations and orientations to reconstruct the photographed scene [24]. This type of topographic survey technique is made possible by recent advances in computer vision. Compared to traditional photogrammetry, SfM uses algorithms to identify matching features in a collection of overlapping digital images and calculates camera location and orientation from the differential positions of multiple matched features [12]. The software aligns the images collected to generate a 3D point cloud model of the photographed object or surface area. This is often a very time-consuming process, depending on the size of the data being processed and the system resources available. The use of GCPs is required to georeference the products with known coordinates in order to develop accurate digital surface models [22]. One of the limitations to SfM photogrammetry is the time-consuming survey of GCPs. There can also be challenges involved with shadows in the imagery, and the time it takes to locate the GCPs in the captured images. To overcome some of these challenges LiDar has been explored in certain mapping applications, however it still falls short of SfM photogrammetry due to the cost and complexity of the data processing.

Applications. As advances to SfM Software have been made, it has become a more powerful and sophisticated tool. It is a low-cost, user-friendly photogrammetric technique that allows high-resolution datasets at a range of scales. The techniques used give users the ability to process imagery of varying resolutions and with variable levels of overlap. This provides an ideal process for imagery acquired from sUAS platforms. There is evidence that there is a relationship between the number and distribution of GCPs needed for accurate georeferencing which is relevant to the SfM process. A study conducted on SfM as a low-cost, effective tool for

geoscience applications used the application of SfM on three contrasting landforms across a range of scales including: an exposed rocky coastal cliff, a breached moraine-dam complex, and a glacially sculpted bedrock ridge [19]. The study revealed that it is possible to reach decimeter-scale vertical accuracy for field sites that cover complex topography and have a variety of land covers. In addition, others also investigate the application of SfM in various other fields of discipline such as geophysics, geology, and geomorphology [1]. Photogrammetry has also proven itself useful for tasks such as landscape studies, which include, but are not limited to, mapping archaeological sites [13]. One challenge that all of these studies face is the ultimate decision to make regarding the number and spatial distribution of ground control points (GCPs) to use for their particular study site. By evaluating the relationship between the number and distribution of GCPS needed for accurate georeferencing, this challenge could be eliminated.

Ground Control Points

Ground Control Points (GCPs) are essential to aerial mapping. They are used to provide points on the ground that are clearly visible in the imagery and have known spatial coordinates [25]. **Figure 2** is an example of a GCP out in the field with a drone on it ready for takeoff. Without the use of GCPs the reconstruction of the imagery could have errors in the scale and orientation, as well as incorrect absolute position information. The GCP coordinates are measured using traditional surveying methods, such as the use of the Global Navigation Satellite System (GNSS). While all the points in the field are used as some type of ground control, about 80% are typically designated as GCPs used for reconstruction, and the remaining 20% are used as checkpoints (CPs). The CPs were only used for evaluating error between the variations of GCPs used in each trial.

Figure 2. Canvas Ground Control Point in the Field Used for Georeferencing

A typical GCP that is used in field mapping is a canvas sheet with a checkerboard pattern that is easily portable and can be staked down, as shown in **Figure 2**. While the use of a recognizable pattern such as the checkerboard is preferred, a GCP is anything that is easily identified in the images. Manholes and parking stripes are examples of photo identifiable GCPs that can be surveyed at any time [25]. There are also disposable GCP options such as the one shown in **Figure 3**.

Figure 3. A Visible and Cost-effective GCP used for sUAS Mapping Applications that is 100% Biodegradable in 3-6 Months

Every survey or study that is conducted can take a considerable amount of time. While some may only take a couple people, others can take multiple crews to lay out, survey, and retrieve the GCPs. Depending on the workforce available and the size of the field site, the time necessary could be multiplied by hours, if not days. A study done to determine the effect of GCP quantity on DEM accuracy in sUAS-based SfM photogrammetry determined that a 0.60 ha field site with variations in relief, topography, and natural and human-made features was accurately georeferenced with 5 GCPs [28]. The results from this study also showed that when fewer than 5 GCPs were used, the amount of error in the derived SfM digital surface models (DSMs) and orthophotos rapidly increase. It also indicated that after 5, any additional GCPs could result in more accurate DEMs, but that the overall gains were relatively minor. Another study found that the optimal number of GCPs for small and medium sites, categorized as 7-39 ha by the research, found that 12 GCPs were necessary based on the overall accuracy [18]. The spatial distribution of the GCPs across the study area is also significant. Previous studies have shown that it is necessary to place some of the GCPs around the edge of the study area to minimize planimetry errors and use a stratified distribution inside of the study area with other GCPs to minimize altimetry errors [27]. The Nevada Department of Transportation utilized the Pix4Dmapper photogrammetry software to do a study that found placing more than 5 to 10 GCPs has little added benefit on the accuracy of the products [23]. Another study showed that the RMSE was reduced to 50% with an increase from 4 to 20 GCPs, but any additional GCPs only slightly improved the results [30].

Each of these studies reports in the range of 4 to 12 GCPs, with any additional having little added benefit on the accuracy of the final products. However, this range still leaves a considerable gap in the number of GCPs that should be used. While the use of GCPs for

accurately georeferencing field sites has proven to be beneficial, the workload to deploy, survey, and collect numerous GCPs can be difficult and laborious [29]. The processing time is also increased as more time must be spent marking GCPs in the software, although this task can easily be completed by one person. By reducing the number of GCPs that are needed in the field, you are able to cut down the portion of the operation that takes up the largest amount of time, resulting in time and cost savings.

Objective

The objective of this research was to determine the optimal number and spatial distribution of ground control points (GCPs) to accurately georeference field sites for SfM photogrammetry. This was done by assessing the relationship between DSM accuracy and the optimal number and configuration of GCPs. By determining a relationship between the level of desired accuracy in relation to the topography and land cover of a particular field site, the surveyor will have the ability to minimize the necessary investment of time and effort involved in deploying GCPs. This will also maximize the accuracy of the SfM products.

Hypothesis

The literature suggests that there is a relationship between DSM accuracy and the optimal number and configuration of GCPs required to accurately georeference the SfM products. This project was designed to explore this relationship. Multiple trials were compared that each used different numbers and combinations of GCPs to georeference the aerial imagery. It was expected that the georeferencing accuracy in the SfM-derived DSMs would reach in inflection point and continue to increase asymptotically after a particular threshold of GCPs is exceeded.

METHODS

Study Area

Fellows Lake is in the North-central Ozarks and is characterized by a mid-latitude, temperate climate. The landscape around Fellows Lake, near Fair Grove, Missouri, exhibits low to moderate relief. The study area contains a mix of dense hardwood forest, grasslands, and savannah-like vegetation. As such, Fellows Lake is representative of the Ozarks, and more broadly of many temperate, mid-latitude localities.

Geography & Geology. Fellows lake is located north of Springfield, Missouri off Highway 65 as shown in **Figure 4**. It is a 348-ha lake that is the main source of drinking water for Springfield, Missouri. The reservoir is owned by City Utilities of Springfield. Surrounding the NW portion of the lake is the area targeted for this study, which covers about 52 hectares. This area was chosen because it is representative of the Ozarks topography and land cover.

The Ozark Plateaus Physiographic Province, also known as the Ozarks, covers approximately 168,349 Square Kilometers (km^2). This area spans mostly Missouri and Arkansas, but also includes some parts of Oklahoma, Kansas, and Illinois. The Ozark Plateaus Province is underlain by a structural dome which was formed by a series of uplifts that have gradually occurred since Precambrian time [4]. Among the horizontal bedrock are caves, sinkholes, and natural springs. The province is divided into four sub-sections: Salem Plateau, Springfield Plateau, St. Francois Mountains, and the Boston Mountains. The study area at Fellows Lake is part of the Springfield Plateau as shown in **Figure 5** [5]. It consists of an irregular-shaped band of resistant Mississippian carbonates. Limestone and dolomite are the primary composition in this area, along with some shale, sandstone, and chert [17].

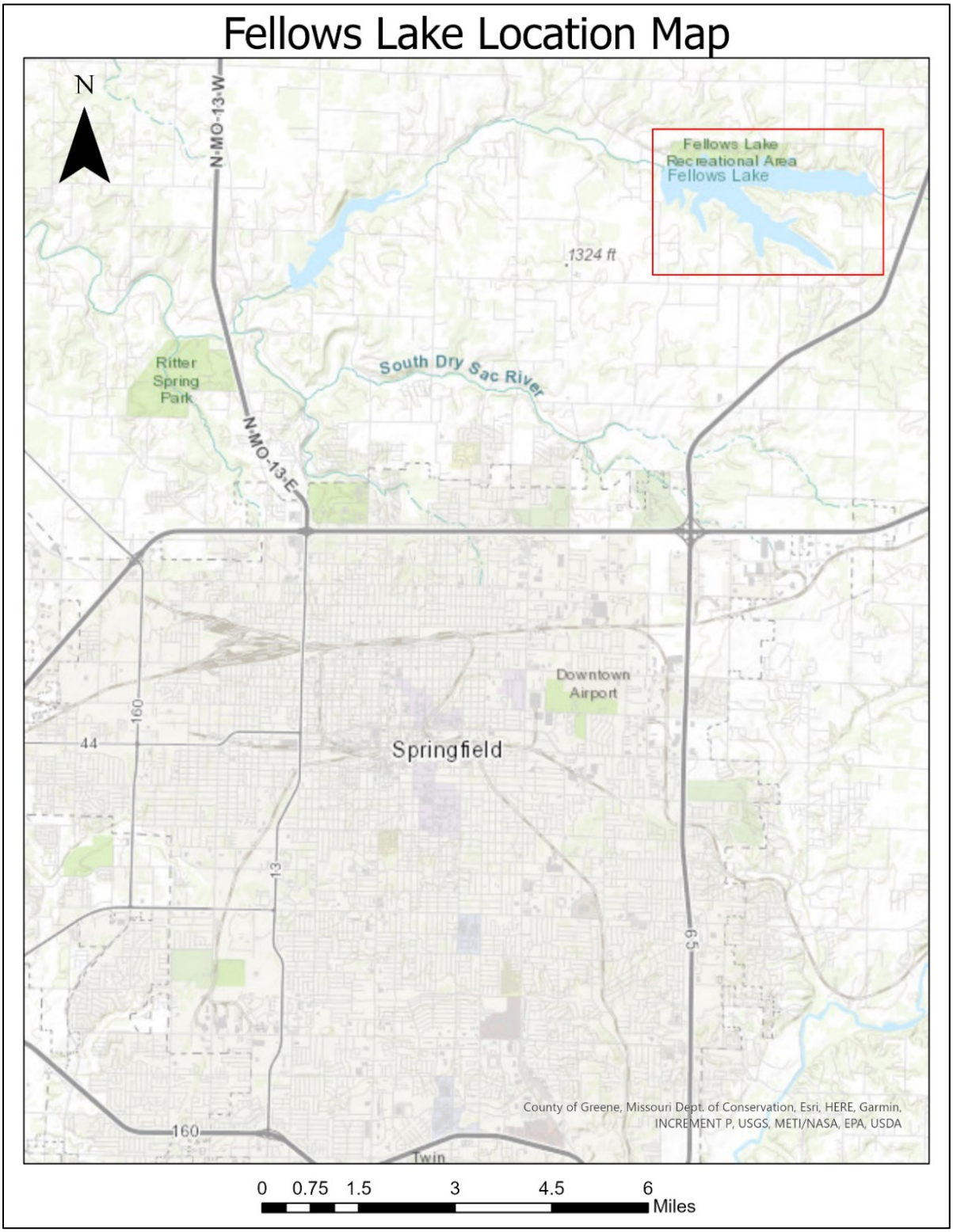

Figure 4. Location Map of Fellows Lake Located North of Springfield, MO

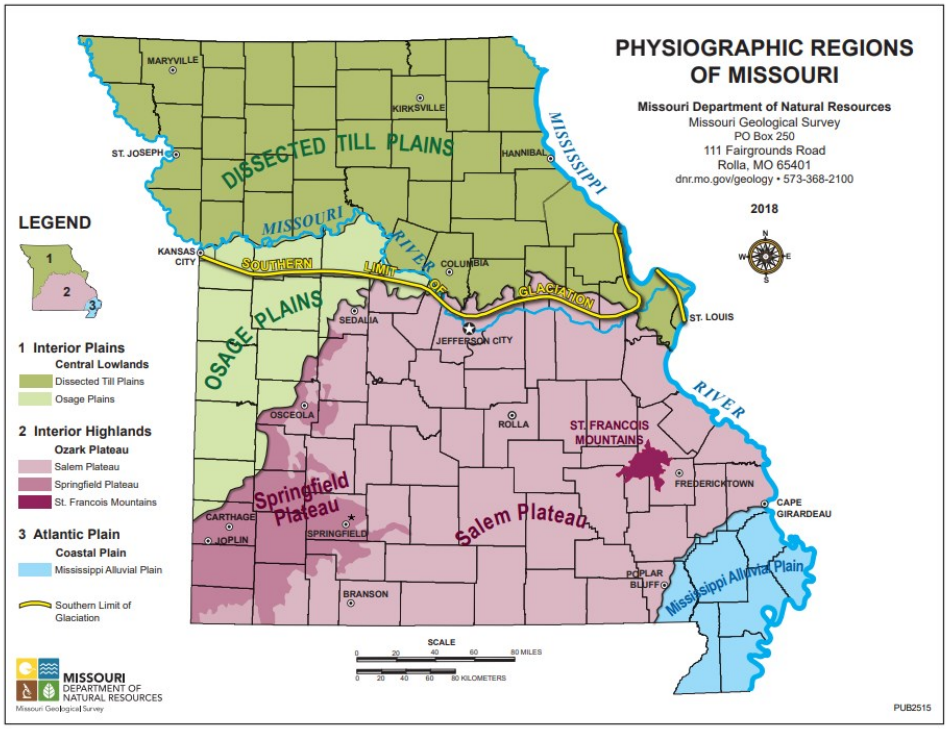

Figure 5. Map of the Physiographic Regions of Missouri

Vegetation. Missouri has nine major types of natural communities: forest, woodland, savanna, prairie, glade, cliff and talus, stream edge, wetland, and cave [3]. The Ozarks vegetation community is dominated by open oak-hickory and shortleaf pine woodlands and forests [2]. The northwest area bordering Fellows Lake is utilized in this project for the mix of woodland, savanna, and prairie. This area can be seen in **Figure 6.** The woodlands at Fellows Lake have relatively open canopies. Large oaks and hickories are the primary components. The savannah forms an intermediate habitat between the woodland and grassland area. The soil conditions at Fellows Lake have a limited depth of fertile soil for grassland vegetation resulting in areas across the field site with surficial bedrock exposure (Fellows Lake Plan, 2020).

Figure 6. Map of Fellows Lake Field Site Area

Field Methods

GCP Deployment. Canvas checkerboard GCPs were selected for this project. They were chosen for their size (1.22 m by 1.22 m) and visibility (black and white pattern), making them easily identifiable in photos from the altitude of 91 (+/-) meters above ground level at which the images were acquired. This visibility makes it possible to accurately mark the GCPs in Metashape during processing.

A total of 21 GCPs were distributed across the field site. Their placement was chosen based on areas that were representative of the field site. This process was based not only on some common sense and experience, but also attention to the changes in ground cover as well as the changes in topographic relief. The locations of these GCPs are shown in **Figure 7**.

Figure 7. Ground Control Point Location Map

To precisely locate the GCPs, centimeter accuracy Post-Processed Kinetic (PPK) GNSS was used. Specifically, the high precision Emlid Reach RS+ GNSS units were used for this project. The Emlid Reach RS+ Survey Kit is shown in **Figure 8**. One of the units was set up as a base station over a temporary benchmark. The base station was located approximately in the center of the study site near the takeoff and landing area. Once the base station was set up, the benchmark coordinates were determined by Precise Point Positioning (PPP) post-processing of raw GNSS data that was collected for multiple hours over the course of a day.

Figure 8. Emlid Reach RS+ GNSS Receiver
A base station and rover setup were used, and the rover positions were corrected using PPK post-processing to accurately locate each control point.

This method of providing positional corrections is known as differential GPS (dGPS). It uses a fixed, known position to adjust the real time GPS signals to eliminate the errors. The post-processed PPP solutions for the benchmark were within decimeter accuracy. The general characteristics of a base station setup with the rover is shown in **Figure 9**. The raw GNSS base

station data was post-processed using the Natural Resources Canada Precise Point Positioning (PPP) web application. The PPP solution utilized the rapid ephemeris and clock data. The final coordinates returned for the base station were used as the absolute reference for post-processing the raw GNSS data collected by the rover units for each of the surveyed GCPs. You can see an example of the rover unit stationed over a GCP collecting data at the Fellows Lake field site in **Figure 10**.

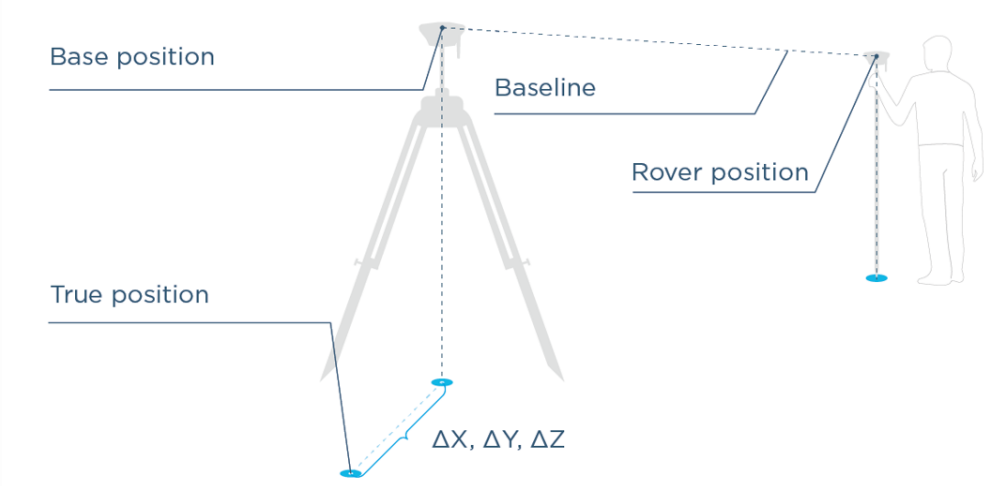

Figure 9. General Base Station Setup
The resulting benchmark coordinates provided the basis of the absolute georeferencing used for the photogrammetry.

The GCPs were surveyed with a rover that recorded the raw GNSS data. The rover units were stationed over each GCP using a bipod and circular level to ensure that the receiver was plumb and stationary during the period when the raw GNSS data was obtained. A minimum of 120 seconds of data were collected at each GCP. The rover data was then post-processed using a post-processed kinematic (PPK) methodology that calculated the corrections based on the raw data that is collected simultaneously by the base station. This was accomplished using the open-source version of RTK Post distributed by Emlid for use with their GNSS receivers.

Figure 10. Rover stationed over a GCP collecting data at Fellows Lake

The final corrected positions for the utilized GCPs had calculated accuracies of 1-3 cm or better. The GNSS-determined elevation of the GCPs used in this study as well as the reported

positional accuracies are shown in **Table 1**. This data was imported from the results of the GNSS post-processing, then Metashape calculated the errors and projections. The imported and calculated information is found in the Reference Pane of Agisoft Metashape. The "Projections" indicates the number of overlapping photos that each GCP was visible in.

Table 1. Imported results of the GNSS post-processing and Metashape calculated errors and projections, found in the Reference Pane of Agisoft Metashape. The number of overlapping photos that each GCP are visible in are indicated by the "Projections" number.

Markers	Longitude	Latitude	Altitude (m)	Accuracy (m)	Error (m)	Projections	Error (pix)
CP (GCP17)	-93.23246158	37.31527718	333.98	0.0059/0.007/0.0145	12.51251035	42	0.889792958
CP (GCP20)	-93.22515475	37.31886722	367.354	0.0043/0.005/0.0099	0.312684696	18	0.907345582
CP (GCP29)	-93.22297528	37.31775115	370.326	0.0303/0.025/0.0602	13.07481097	20	0.865377496
CP (Flagpole)	-93.2276498	37.31797713	361.724	0.0047/0.0051/0.0089	1.082718392	38	2.139481267
GCP01	-93.2351644	37.31891273	331.423	0.0062/0.0074/0.0246	3.247654134	18	0.528122042
GCP02	-93.23428379	37.31815967	324.938	0.0069/0.0081/0.0323	3.544373921	23	0.60712448
GCP03	-93.2305626	37.31771531	333.276	0.0037/0.004/0.0091	0.250357171	21	0.710375268
GCP04	-93.22708591	37.31834756	364.226	0.0048/0.0053/0.0085	0.255889367	45	0.688855241
GCP06	-93.23422955	37.3177548	325.285	0.0196/0.019/0.0367	5.216573739	20	0.326270869
GCP07	-93.22632069	37.31987678	357.24	0.0049/0.007/0.013	0.780298416	11	0.457434293
GCP10	-93.22388706	37.3177629	371.409	0.011/0.01/0.0166	2.4517514	22	0.590898084
GCP11	-93.23123883	37.31645414	335.966	0.0337/0.05/0.0759	7.953569232	35	0.880244003
GCP13	-93.22409472	37.3174985	367.447	0.0183/0.016/0.0259	3.931955373	23	0.81227913
GCP16	-93.22789083	37.31773639	359.473	0.0047/0.0045/0.0098	0.418528547	29	0.642560246
GCP21	-93.22301298	37.31970529	364.238	0.006/0.0164	2.949860386	12	0.988663031
GCP22	-93.22465966	37.31979634	362.232	0.0044/0.005/0.011	0.950269611	11	0.808049392
GCP23	-93.23075052	37.31672092	330.321	0.0059/0.006/0.0155	1.568162302	25	0.834234249
GCP24	-93.22656269	37.31823	364.456	0.0056/0.006/0.0126	0.452373315	50	0.809206182
GCP25	-93.22223816	37.31806097	364.591	0.0069/0.008/0.0261	0.869211931	20	0.697023691
GCP27	-93.22491621	37.31788308	365.549	0.0062/0.007/0.0138	1.177500378	15	1.75E+00
GCP30	-93.23292699	37.31513845	314.182	0.0049/0.005/0.0107	0.037627357	42	0.675821486

Flight Plan. A DJI Phantom 4 Professional sUAS was used to acquire the imagery for the SfM photogrammetry. For this project, a flight mission with 80% side and forward image overlap was chosen. In theory only 50-60% front and side overlap are adequate, however in practice results have shown that it takes 70% or more for successful photogrammetry. The

mission was flown at an altitude of 91 (+/-) meters above ground level (AGL) with a target resolution of 2.5 cm/px was flown in an EW "lawnmower" pattern. An orthogonal camera angle was chosen (i.e., straight down). Map Pilot for Business by Maps Made Easy was used as the mission planning and flight control software. The Terrain Aware setting in Map Pilot was used so that the drone adjusted its altitude and positioning automatically by analyzing the terrain so that it could maintain the same flight altitude AGL for the entire image acquisition process. By maintaining the same flight altitude, the resolution on the aerial images collected is more consistent. The flight covered an area of approximately 52 hectares. The plot at the bottom of **Figure 11** shows the profile of the flight line as the drone crossed back and forth across the upland area and over the valley.

Data Processing

Following the flight, the acquired imagery was processed using Agisoft Metashape. This software has the capability to run multiple trials, each with unique variations of ground control points (GCPs). Each trial produced a dense cloud, Digital Surface Model (DSMs), and orthomosaic. The number of GCPs, and which specific ones were used for each trial are listed in **Table 2**. A unique variation of GCPs were selected with respect to elevational and land cover changes, along with their spatial distribution across the field site for each trial.

The selection of GCPs was a critical part in the process. A total of 21 GCPs were placed across the field site. They were placed across the field site with respect to the elevational and land cover changes. Prior to going out into the field, a GCP location plan was made by looking at the area in google earth. This made it possible to determine what type of land cover could be expected across the field site and where the GCPs should be placed.

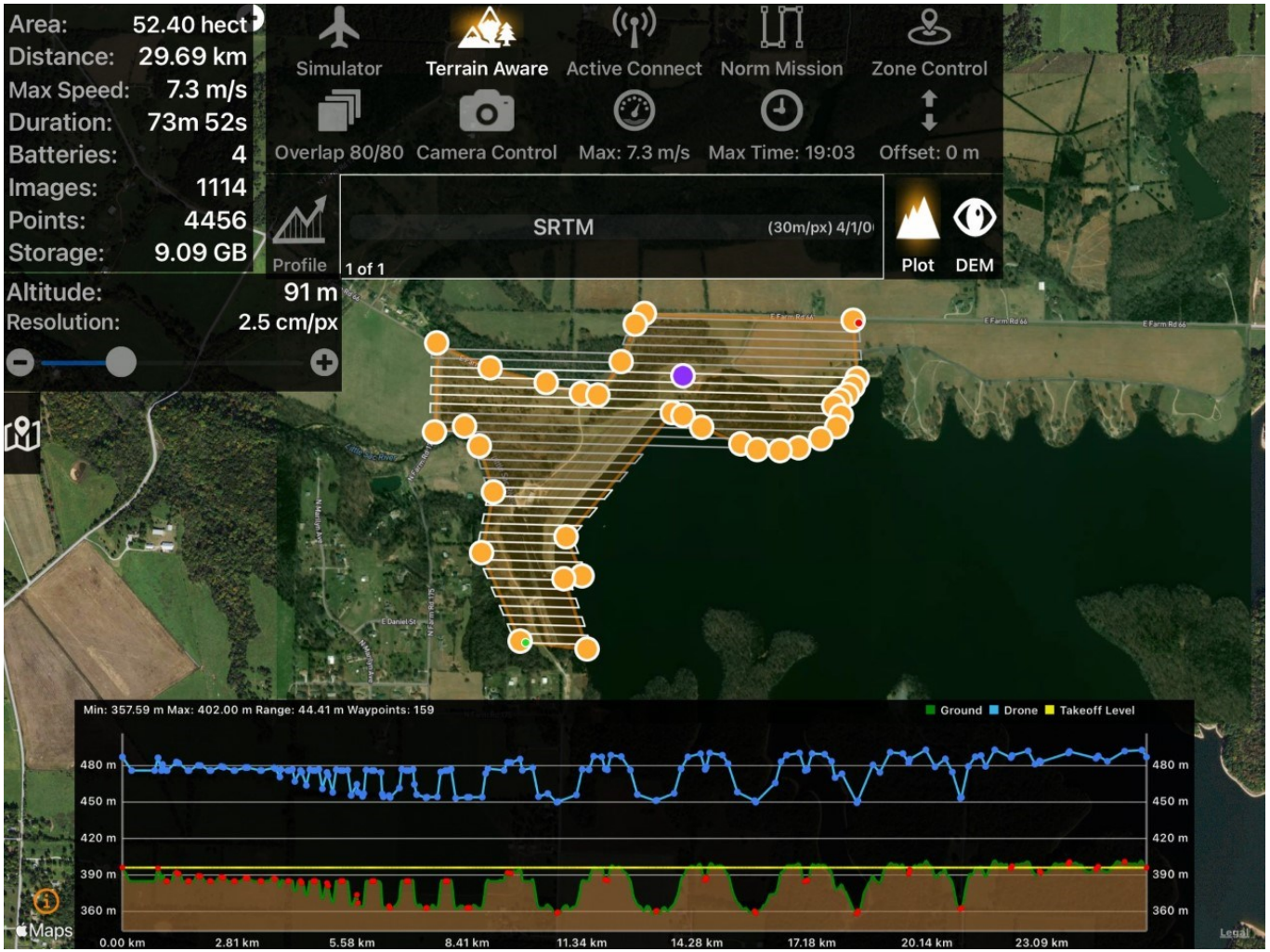

Figure 11. Screenshot of the Fellows Lake Flight Mission

Table 2. Ground Control Points Utilized Per Trial

# of GCPs	Trial 1	Trial 2	Trial 3	Trial 4	Trial 5	Trial 6	Trial 7	Trial 8	Trial 9	Trial 10	Trial 11	Trial 12
0	No GCPs											
1		16	02	01	02	01	01	01	01	01	01	01
2			25	22	03	03	03	03	03	02	02	02
3				30	16	04	04	04	04	03	03	03
4					25	22	07	07	07	04	04	04
5						30	16	16	16	07	07	06
6							22	21	21	16	10	07
7							30	22	22	21	13	10
8								23	23	22	16	11
9								30	24	23	21	13
10									27	24	22	16
11									30	25	23	21
12										27	24	22
13										30	25	23
14											27	24
15											30	25
16												27
17												30

For example, as you can see in **Figure 7**, there are GCPs located in the open areas with higher visibility, and also some placed into the areas with more tree canopy and ground cover. The GCPs were also placed around the parameter of the field area, as well as across the inside of the area, with attention to changes in relief. Specific markers that remained unused were available to be treated as assessment points. These assessment points, also known as Checkpoints (CPs), were only used to evaluate the accuracy of the DSMs. They were never used as GCPs. While you can use any remaining GCPs as CPs, this study used the same consistent set of 4 CPs to analyze the error. This was done by exporting the DSMs to ArcMap (v. 10.5). Once in ArcMap the elevational values were extracted from the x,y location on the DSM. These extracted DSM elevation values were then compared to the known elevations for that point from the collected GNSS data.

SfM Workflow. SfM software allows for the use of GCPs, measurements, DEM exports, and georeferenced orthomosaic exports. These are all necessary to the methodology that was used to test the ideal number and spatial distribution of GCPs that are needed to optimize the georeferencing accuracy in sUAS based SfM photogrammetry. The United States Geological Society (USGS) published an Agisoft PhotoScan Workflow that is based on the Agisoft Photoscan Professional – Version 1.2.6 build 2834 [20]. This workflow contains the standardized choice of setting and parameters to follow for the photo setup, alignment, adjustment, error reduction and bundle adjustment, along with guidance on the appropriate user options to choose during the processing for building the dense point cloud, DEMs, and orthomosaics, which are all crucial steps in the process of creating high quality maps.

Once the imagery from the flight was loaded into Metashape, the photos were first aligned and then the software generated the sparse point cloud for those images. The images then underwent a Gradual Selection procedure. This procedure is used to remove points with high error values, reducing the errors in the adjustment. If the point's error exceeded a specific threshold, it was selected and deleted. The Reconstruction Uncertainty process which is part of the Gradual Selection tool was first used to remove the points of error that were due to poor geometry. This process was used to get the best data out of the point cloud. Once the points were deleted, the Optimize Camera Alignment tool was used to optimize the camera locations. Once that was completed, the Projection Accuracy process which is another part of the Gradual Selection tool was used to remove points of error due to pixel matching errors. The Optimize Camera Alignment tool was used again after the points were deleted. Once that was done processing, the next step was setting the markers. In the reference panel under the markers list, you can see the list of the GCPs that were previously surveyed at the field site and then added to

the model to increase the georeferencing accuracy of the final products. By right clicking on the individual GCP in the markers list and selecting to filter photos by markers, Metashape shows all the photos that it thinks include that GCP in the photos console. By double clicking on the photos in the console individually it shows where Metashape suggests that the marker be placed. Each marker was manually moved directly to the center of the GCPs for each individual photo. Once all the markers were set, Reprojection Error, another process of the Gradual Selection tool, was used to remove the points of error due to pixel residual errors. Once the Gradual Selection procedure was completed, the cameras were all unchecked. It was at this point that the GCP markers that were being used for that specific trial were selected. **Table 2** shows which GCPs were used per trial. Once the selections were made, the dense point cloud was built for each trial. This procedure assigned color values to accurately create the model [20]. Using the dense point cloud, the DSMs were then constructed.

DSM Analysis. Once the imagery has been processed using Agisoft Metashape, the resulting Digital Surface Models (DSMs) were exported for further analysis. The exported DSMs were then analyzed for a comparison of accuracy. Checkpoints (CPs) were left unchecked within the reference workspace window of Metashape in all the trials ran. By leaving them unchecked they are not used in processing, but the accuracy of the marker is still given, yielding a known 3D point in space without influencing the solution [10]. These four CPs were utilized to aid in the evaluation of accuracy. Differences between the GCP elevation values extracted from the DSMs and the known surveyed positions represent the accuracy with which SfM was able to reconstruct the topography of the area and its features based on the specific GCPs used during the processing.

Elevational Root Mean Square Errors (RMSE) were computed for each of the 12 trials. The equations for these calculations are shown in **Figure 12**. RMSE measures the average magnitude of the error based on the square root of the average of squared differences between the DSM predicted elevations and the actual surveyed elevations. These values were then compared to Mean Absolute Error (MAE) calculations. MAE also measures the average magnitude of the errors; however, it is the average of the absolute differences between predicted and actual observations where all the individual differences have equal weight. By using RMSE and MAE together you can find the variation in the errors. The greater the difference between them, the greater the variance in the individual errors in the sample. If RMSE were to equal MAE, then all the errors would have the same magnitude.

$$\text{RMSE} = \sqrt{\frac{\sum_{i=1}^{n}(e_i)^2}{n}}$$

$$\text{MAE} = \frac{\sum_{i=1}^{n}|e_i|}{n}$$

Figure 12. RMSE & MAE Equations

RESULTS

An overall error analysis comparing the RMSE and MAE which were calculated using the elevation (z) values for all 12 trials is shown in **Figure 13**. Here you can see the number of GCPs used in each trial, and how that number relates to the level of error in the DSMs produced. There is a noticeably clear influence that the use of GCPs has on the level of accuracy.

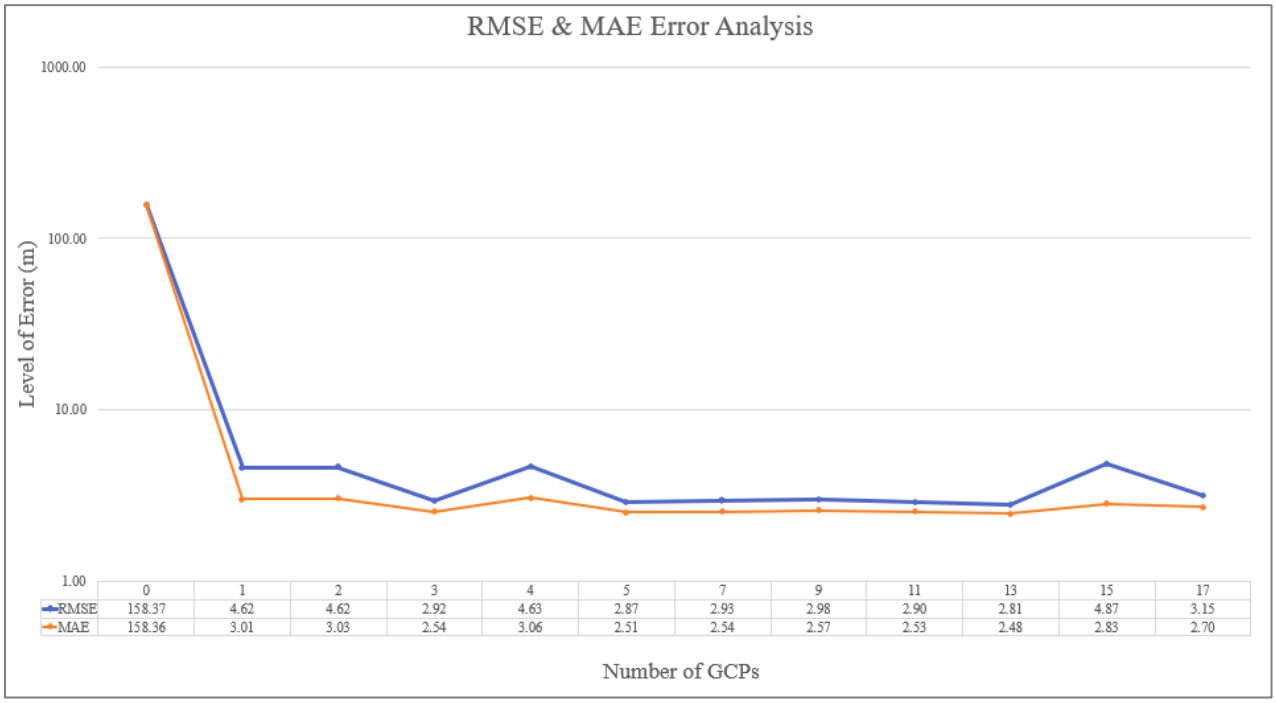

Figure 13. Results of the RMSE & MAE Error Analysis per Trial

To take a closer look at the influence that the number of GCPs had on the level of RMSE and MAE error values, the trial that did not use any GCPs was removed from the comparison. **Figure 14** shows the RMSE & MAE error values for the 11 trials that utilized GCPs to increase the DSM accuracy. Aside from the trial which used 15 GCPs, there was not a notable change in

the level of error when any more than 5 GCPs were used. This indicates that 4 GCPs is the threshold. There would not be an advantage to using any additional GCPs past this point to make an impact on the level of accuracy.

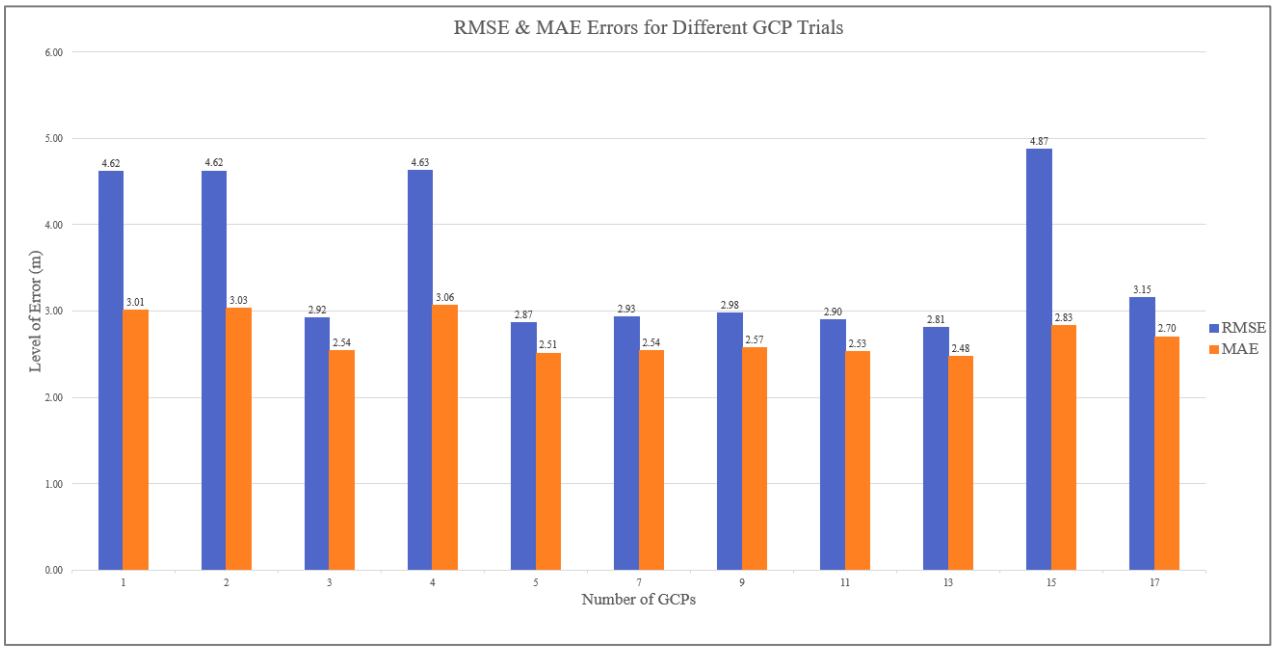

Figure 14. RMSE & MAE Error Values for Trials with GCPs Utilized to Increase DSM Accuracy

To further assess the accuracy of the DSMs, the level of error in the easting (x), northing (y), vertical (z), horizontal (xy), and 3-dimensonal (xyz) values were also calculated. Using a combination of error assessments was suggested in the paper, Accuracy of Digital Surface Models and Orthophotos Derived from Unmanned Aerial Vehicle Photogrammetry, where the influence of flight altitude, terrain morphology and the number of GCPs on DSMs and orthoimagery obtained by sUAS was explored [7]. A study which assessed the accuracy of the use of sUAS and SfM photogrammetry to generate DSMs for open-pit coal mine areas contained the equations used to calculate each type of RMSE is shown in **Figure 15** [8].

$$RMSE_{X} = SQRT\left[(1/n)\sum_{i=1}^{n}(X_{DSM} - X_{GCPi})^2\right]$$

$$RMSE_{Y} = SQRT\left[(1/n)\sum_{i=1}^{n}(Y_{DSM} - Y_{GCPi})^2\right]$$

$$RMSE_{Z} = SQRT\left[(1/n)\sum_{i=1}^{n}(Z_{DSM} - Z_{GCPi})^2\right]$$

$$RMSE_{XY} = SQRT\left[(1/n)\sum_{i=1}^{n}((X_{DSM} - X_{GCPi})^2 + (Y_{DSM} - Y_{GCPi})^2)\right]$$

$$RMSE_{XYZ} = SQRT\left[(1/n)\sum_{i=1}^{n}((X_{DSM} - X_{GCPi})^2 + (Y_{DSM} - Y_{GCPi})^2 + (Z_{DSM} - Z_{GCPi})^2)\right]$$

Figure 15. Equations for calculating one-dimensional RMSE (for individual X, Y, and Z coordinates), two-dimensional RMSE (for X, Y coordinates), and three-dimensional RMSE (for X, Y, and Z coordinates).

The RMSE analysis for the level of Z errors, XY errors, and XYZ error was calculated by following this methodology. The results can be seen in **Figure 16**. The influence of GCPs can again be seen by looking at the first trial with the highest level of all error values that did not use any GCPs. You can also see how past the threshold of 4 GCPs, each type of error levels out once 5 GCPs are used. This is with the exception of the outlying group that used 15 GCPs.

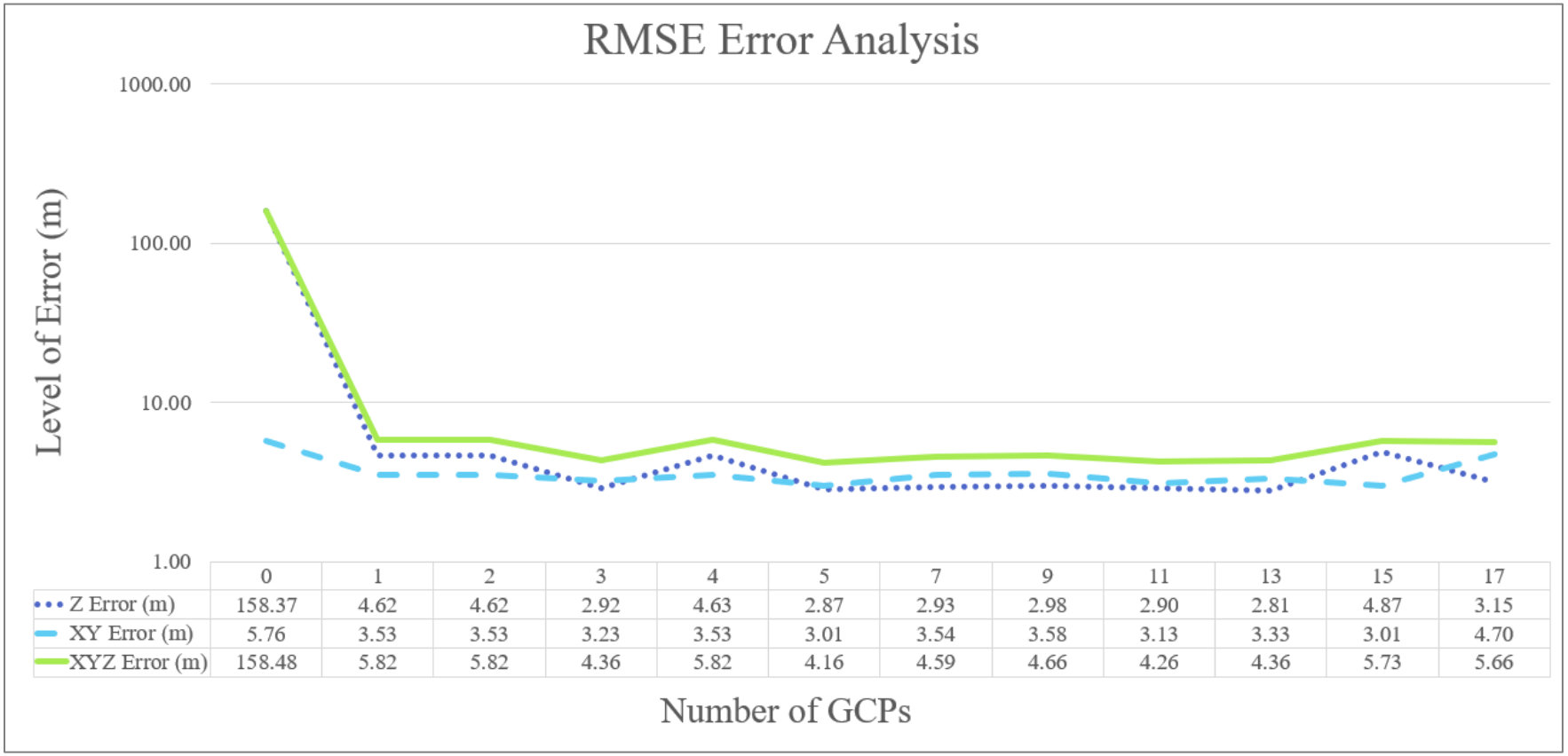

	0	1	2	3	4	5	7	9	11	13	15	17
Z Error (m)	158.37	4.62	4.62	2.92	4.63	2.87	2.93	2.98	2.90	2.81	4.87	3.15
XY Error (m)	5.76	3.53	3.53	3.23	3.53	3.01	3.54	3.58	3.13	3.33	3.01	4.70
XYZ Error (m)	158.48	5.82	5.82	4.36	5.82	4.16	4.59	4.66	4.26	4.36	5.73	5.66

Figure 16. Vertical ($RMSE_Z$), Horizontal ($RMSE_{XY}$), and 3D ($RMSE_{XYZ}$) Error Analysis

DISCUSSION

In the process of determining the optimal number of GCPs to accurately georeference DSMs derived from sUAS-based SfM photogrammetry, it was found that using more than 5 GCPs did not result in a notable change in the DSM accuracy as measured by RMSE and MAE. These results are applicable to sites with similar characteristics to the Fellows Lake site: low to moderate relief, mid-latitude, temperate climate, with a mix of forest, grasslands, and savannah. The results from this study, along with those from a much smaller field site [28], but with otherwise similar characteristics, suggest that the number of GCPs necessary to georeference a site does not vary with site size, at least within the range of <1 ha to 52 ha. It could also be possible that while three GCPs is the minimum needed mathematically for SfM photogrammetry, there could be other factors influencing the level of error. The drone specifications (photo quality, resolution, image blur, flight plan, etc.) and the processing methodology (error reduction), or the software's ability to estimate the scale with fewer GCPs could all be impacting the results. Thus, it could be the acquisition hardware and processing methodology that have a greater influence on determining the GCP requirements. This could explain how results were obtained when only using 1 or 2 GCPs. The trial that uses 15 GCPs is another outlier. It could be beneficial to see if this could be resolved by testing multiple trials that use different combinations of 15 GCPs as well and see how they compare. While 5 GCPs seems to be a sufficient amount for Metashape to accurately georeference a wide range of field sites, the required level of accuracy is dependent on the objectives of individual projects. Determining a relationship between the level of desired accuracy in relation to the topography and land cover of a particular field site will maximize the accuracy of

the SfM products. While I was able to reproduce comparable results for a significantly larger field site, the terrain characteristics, size, equipment, and processing methodologies could have all contributed to making these results possible.

Other investigators have found that a greater number of GCPs are necessary to optimize the accuracy of DSMs derived from SfM-based photogrammetry [14,11]. For example, a study done to determine the optimal number of ground control points for varying study sites through accuracy evaluation of unmanned aerial system-based 3D point clouds and digital surface models found that 12 GCPs were required to georeference what they categorized as small and medium sites (7 and 39 ha), and 18 GCPs for the large sites (342 ha) [18]. These sites consisted of a small aggregate yard, coastal area, and an industrial complex in a metropolitan city. The small site did not have any vegetation on the ground surface, the medium site was composed of tidal flats with no vegetation, and the large site again contained no vegetation and was covered with buildings, pavements, and sidewalk. While these field sites were covered a variety of terrain characteristics, there were no extreme changes in the topography or relief compared to the Fellows Lake field site. The main difference between the projects being the Metashape processing workflow which was much more condensed than the workflow followed for this project. It depended heavily on the Metashape software to complete the following steps: camera calibration-align–absolute orientation–camera align optimization–3D point cloud generation–DSM generation. This methodology did not utilize the use of gradual selection to help reduce the level of error prior to the DSM construction. It is possible that differences in the methodology is what resulted in the need for a higher number of GCPs to model the various areas. Likewise, another study done to determine the suitable number of ground control points for sUAS images georeferencing by varying number and spatial distribution found that the RMSE could be reduced down to 50%

when switching from four to 20 GCPs and using higher numbers of GCPs would only slightly improve the results [15]. This study chose to fly a 0.8 ha area that consisted of several land uses to represent both artificial surfaces (building roofs, parking lots, roads) and natural surfaces (green area). This study again followed a considerably different workflow for processing the imagery that was collected. The imagery was processed using 3DF Zephyr Pro software which makes an approximation for the interior and exterior orientation parameters for each camera position. All 300 GCPS and CPs used in the project then had to be manually measured on each oriented image that they appeared on, with a minimum of 3. A bundle block adjustment was performed to bring the results into the desired coordinate system, which only included the GCPs as constraints, while the other points served as checkpoints. For each scenario, a dense point cloud with a mesh surface was automatically generated. The difference in the processing methodology could again be the key component to producing higher levels of error compared to this project which was able to produce much lower error levels in the accuracy assessment of the georeferencing process. Even as these previous studies have suggested that the number of GCPs required to optimize DSM accuracy varies with the size of the study site, our data suggest this is not the case.

Future Work. Upon analyzing the results of the 11 trials that used GCPs, there are some possibilities for future work. It is interesting that the trial using only three GCPs would have such a low level of error (and that trial 11, which used 15 GCPs had a much higher error than all the other trials with more than 5 GCPs). By testing multiple combinations of three and 15 GCPs it would be possible to see if these errors are anomalous or if those specific sets of GCPs happened to cause a different error than other sets with the same number of GCPs. This could suggest that

GCP distribution across the site or across variations in topography or vegetation is also important in optimizing DSM accuracy.

It would also be beneficial to see how these results apply to a broader range of field sites. Would 5 GCPs be capable of producing the same results in an area that has more complex topography such as steep cliffs? Field settings with higher relief may require different mission planning. It could be that 5 GCPs is adequate, but the guidelines on how to place them could differ. Exploring the size of the field site in relation to the results also offers another avenue to test these results. Because only ground based GCPs were used in this study it is unclear how accurately the heights of trees or other vegetation are represented within the DSM (in comparison to "bare earth" elevations).

Summary. A SfM photogrammetry dataset was processed with twelve different trials each using a different number of GCPs. The accuracies of the DSMs resulting from each trial were compared based on their RMSEs and MAEs. It was found that the level of accuracy in the SfM products did not change significantly with more than 5 GCPs. These results are comparable to a previous study where similar conclusions were reached for a 0.60 ha field site [28]. This suggests that GCP requirements do not vary with site size, at last in the range of <1 to 50 ha.

These findings provide guidance on the use of GCPs in georeferencing sUAS-based photogrammetry products. Because GCP deployment, surveying, and retrieval are typically the most time-consuming part of UAS-based photogrammetry data acquisition, determining the threshold for the number of GCPs required to optimize DSM accuracy will ensure the efficiency and cost-effectiveness of SfM projects.

REFERENCES

1. Nyimbili, P.; Demirel, H.; Seker, D.; Erden, T. Structure from Motion (SfM) - Approaches and Applications 2016. Available online: https://www.researchgate.net/publication/327630010_Structure_from_Motion_SfM_-_Approaches_and_Applications

2. USGS The Ozark Highlands 2009. Available online: https://pubs.usgs.gov/fs/2009/3065/pdf/FS2009-3065.pdf

3. MDC Terrestrial Natural Communities of Missouri 2010. Available online: https://nature.mdc.mo.gov/discover-nature/habitats/statewide-habitat-systems/terrestrial-natural-communities-missouri (accessed on Apr 7, 2021).

4. USDA Ouachita National Forest - Land & Resources Management 1999. Available online: https://www.fs.usda.gov/detail/ouachita/landmanagement/?cid=fsm9_039810 (accessed on Jun 18, 2021).

5. DNR Springfield Plateau Groundwater Province 2016. Available online: https://dnr.mo.gov/geology/wrc/groundwater/education/provinces/springfieldplatprovince.htm (accessed on Apr 7, 2021).

6. DJI Official DJI Phantom 4 Pro – Specs, Tutorials & Guides – DJI 2016. Available online: https://www.dji.com/phantom-4-pro/info#specs.

7. Agüera-Vega, F.; Carvajal-Ramírez, F.; Martínez-Carricondo, P. Accuracy of Digital Surface Models and Orthophotos Derived from Unmanned Aerial Vehicle Photogrammetry. *Journal of Surveying Engineering* **2017**, 143, 04016025, doi:10.1061/(ASCE)SU.1943-5428.0000206.

8. Bui, D.; Long, N.; Bui, X.-N.; Nghia, N.; Chung, P.; Canh, L.; Thao, N.; Bui, D.; Kristoffersen, B. Lightweight Unmanned Aerial Vehicle and Structure-from-Motion Photogrammetry for Generating Digital Surface Model for Open-Pit Coal Mine Area and Its Accuracy Assessment. *In*; **2017**; p. 18 ISBN 9783319682402.

9. Burchfield, D.R.; Petersen, S.L.; Kitchen, S.G.; Jensen, R.R. sUAS-Based Remote Sensing in Mountainous Areas: Benefits, Challenges, and Best Practices. *Papers in Applied Geography* **2020**, 6, 72–83, doi:10.1080/23754931.2020.1716385.

10. Hostens, D. Determining the Effect of Mission Design and Point Cloud Filtering on the Quality and Accuracy of SfM Photogrammetric Products Derived from sUAS Imagery. *MSU Graduate Theses* **2019**.

11. Wolf, P.R.; Dewitt, B.A.; Wilkinson, B.E. Introduction. In Elements of Photogrammetry with Applications in GIS, Fourth Edition; McGraw-Hill Education, 2014 ISBN 9780071761123.

12. Carrivick, J.L.; Smith, M.W.; Quincey, D.J. Structure from Motion in the Geosciences | Wiley Online Books 2016. Available online: https://onlinelibrary.wiley.com/doi/book/10.1002/9781118895818 (accessed on May 4, 2021).

13. O'Driscoll, J. Landscape applications of photogrammetry using unmanned aerial vehicles. *Journal of Archaeological Science: Reports* **2018**, 22, 32–44, doi:10.1016/j.jasrep.2018.09.010.

14. Villa, T.F.; Gonzalez, F.; Miljievic, B.; Ristovski, Z.D.; Morawska, L. An Overview of Small Unmanned Aerial Vehicles for Air Quality Measurements: Present Applications and Future Prospective Sensors 2016, 16, 1072, doi:10.3390/s16071072.

15. Villareal, M.K.; Tongco, A.F.; Maja, J.M.J. Winter Wheat Crop Height Estimation Using Small Unmanned Aerial System (sUAS) 2020. Available online: https://www.scirp.org/journal/paperinformation.aspx?paperid=99297 (accessed on Apr 16, 2021).

16. Martinez, J.G.; Albeaino, G.; Gheisari, M.; Issa, R.R.A.; Alarcón, L.F. iSafeUAS: An unmanned aerial system for construction safety inspection. *Automation in Construction* **2021**, 125, 103595, doi:10.1016/j.autcon.2021.103595.

17. NPS Ouachita and Ozark Plateaus Provinces (U.S. National Park Service) 2018. Available online: https://www.nps.gov/articles/ouachitaandozarkplateaus.htm (accessed on Apr 7, 2021).

18. Yu, J.J., Kim, D.W., Lee, E.J., Son, S.W. Determining the Optimal Number of Ground Control Points for Varying Study Sites through Accuracy Evaluation of Unmanned Aerial System-Based 3D Point Clouds and Digital Surface Models. *MDPI* **2020**.

19. Westoby, M.J., Brasinton, J., Glasser, N.F., Hambrey, M.J., Reynolds, J.M. 'Structure-from-Motion' photogrammetry: A low-cost, effective tool for geoscience applications. *ScienceDirect* **2012.**

20. USGS Agisoft PhotoScan Workflow 2017. Available online: https://uas.usgs.gov/nupo/pdf/USGSAgisoftPhotoScanWorkflow.pdf.

21. Fonstad, M.A.; Dietrich, J.T.; Courville, B.C.; Jensen, J.L.; Carbonneau, P.E. Topographic structure from motion: a new development in photogrammetric measurement. *Earth Surface Processes and Landforms* **2013**, 38, 421–430, doi:https://doi.org/10.1002/esp.3366.

22. Goldstein, E.B.; Oliver, A.R.; deVries, E.; Moore, L.J.; Jass, T. Ground control point requirements for structure-from-motion derived topography in low-slope coastal environments; *PeerJ PrePrints*, **2015**. Available online: https://doi.org/10.7287/peerj.preprints.1444v1

23. Pix4d Do more GCPs equal more accurate drone maps? 2018. Available online: https://www.pix4d.com/blog/GCP-accuracy-drone-maps.

24. Shervais, K. Structure from Motion Introductory Guide 2015. Available online: https://www.unavco.org/education/resources/modules-and-activities/field-geodesy/module-materials/sfm-intro-guide.pdf

25. Abdullah, Q.A. Ground Control Requirement | GEOG 892: Unmanned Aerial Systems 2013. Available online: https://www.e-education.psu.edu/geog892/node/649 (accessed on Jul 29, 2020).

26. Persia, M.; Barca, E.; Greco, R.; Marzulli, M.I.; Tartarino, P. Archival Aerial Images Georeferencing: A Geostatistically-Based Approach for Improving Orthophoto Accuracy with Minimal Number of Ground Control Points. *Remote Sensing* **2020,** 12, 2232, doi:10.3390/rs12142232.

27. Martínez-Carricondo, P.; Agüera-Vega, F.; Carvajal-Ramírez, F.; Mesas-Carrascosa, F.-J.; García-Ferrer, A.; Pérez-Porras, F.-J. Assessment of UAV-photogrammetric mapping accuracy based on variation of ground control points. *International Journal of Applied Earth Observation and Geoinformation* **2018**, 72, 1–10, doi:10.1016/j.jag.2018.05.015.

28. Pfitzner, B.; Dogwiler, T. Determining the Effect of GCP Quantity on DEM Accuracy in sUAS-based Structure-from-Motion Photogrammetry. In Proceedings of the Geological Society of America Abstracts with Programs; Indianapolis, Indiana, 2018; Vol. 50.

29. Ren, H.; Zhao, Y.; Xiao, W.; Wang, X.; Sui, T. An Improved Ground Control Point Configuration for Digital Surface Model Construction in a Coal Waste Dump Using an Unmanned Aerial Vehicle System. *Remote Sensing* **2020**, 12, 1623, doi:10.3390/rs12101623.

30. Oniga, V.-E.; Breaban, A.-I.; Pfeifer, N.; Chirila, C. Determining the Suitable Number of Ground Control Points for UAS Images Georeferencing by Varying Number and Spatial Distribution. *Remote Sensing* **2020**, 12, 876, doi:10.3390/rs12050876.